

High-accuracy Hall-based sensors for high magnetic field applications

Vincent Mosser,

Itron Technology Center,
92190 Meudon, France

The logo for Itron, featuring the word "Itron" in a bold, red, italicized sans-serif font. A yellow triangle is positioned above the letter 'o'.

Rémi Boucher,

CAYLAR,
91140 Villebon,
France



Enrique Minaya

CNRS – Institut de
Physique Nucléaire Orsay,
91404 Orsay, France



IMMW21

Grenoble, 24-28 June 2019

- **The Hall effect**
- **Parasitic effects in Hall measurements**
- **2D Quantum Well Hall Sensors vs 3D sensors**
- **QWHS for micromagnetometry - Applications and results**
- **The Spinning Current Modulation Technique (SCMT)**
- **Results at high magnetic field (0 to 7 T)**
- **Conclusion**

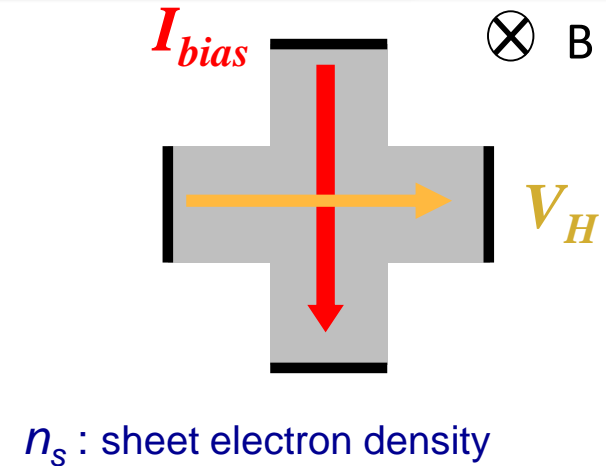
Hall effect in a planar device

- Lorentz force acting on the moving electrons in the channel:

→ transverse electric field $\vec{F} = e\vec{v} \wedge \vec{B}$

- Basic classical Drude-like model:

→ **Hall voltage** $V_H = K_H I B_{\wedge} = \frac{I B_{\wedge}}{en_s}$



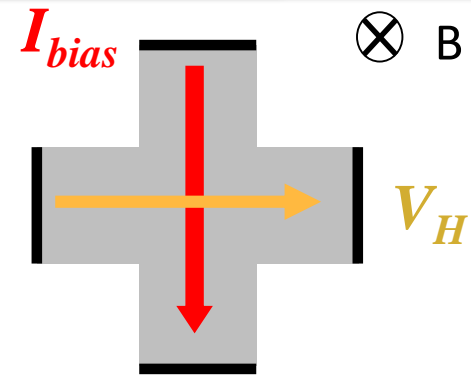
Hall effect in a planar device

- Lorentz force acting on the moving electrons in the channel:

→ transverse electric field $\vec{F} = e\vec{v} \wedge \vec{B}$

- Basic classical Drude-like model:

→ **Hall voltage** $V_H = K_H I B_{\wedge} = \frac{I B_{\wedge}}{en_s}$



n_s : sheet electron density

Unwanted parasitic effects

- The Hall sensitivity may not be a constant

$$K_H = G_H (\mu(T)B) \times \frac{r_H(T, B)}{en_s}$$

cf. R. Popovic's book, "Hall Effect Devices"

Sheet electron density n_s
How to keep it constant?

Geometric factor G_H :
Can be fixed with adequate probe layout
Under certain conditions $G_H = 1$

Hall scattering factor r_H
Microscopic effects: *intrinsic NL*
Depends on material and sensor structure, $r_H = 1$ in degenerate material

- Additive parasitic terms in the output signal V_{out}

$$V_{out} = K_H I B_{\wedge} + \text{parasitic terms}$$

Parasitic terms in the output signal V_{out}

- Offset
- Piezoresistance effect
- Non-linearity vs B
- Cross-sensitivity to in-plane $B_{//}$ (PHE = Planar Hall Effect)
- Thermal and temporal drift of offset
- Thermal and temporal drift of sensitivity
- Noise

Their magnitude strongly depends on material and sensor structure

Dynamic cancelation of parasitic terms

- Some of these effects can be canceled out by various techniques, the most powerful is the Spinning Current Modulation Technique (SCMT)
- Again, ***depending on the type of material considered***, SCMT might be more or less powerful in canceling the parasitic effects

Selected material

Quantum Well Hall Sensors (QWHS)

AlGaAs/InGaAs/GaAs

- 2DEG: combines the benefit of a degenerate semiconductor together with a low electron density n_s
- Available from industrial III-V foundries

Materials / schematic structure / 2D vs 3D

**Silicon based
CMOS compatible
(Si)**



Implanted or epitaxial n-type active layer confined by p-type bulk and p+ implant

**High-mobility
3D device
e.g. InSb-based
(III-V)**



Epitaxial highly-doped n-InSb layer confined by S.I. substrate

3D active layer thickness: typ. 100 nm to 2 μm or more

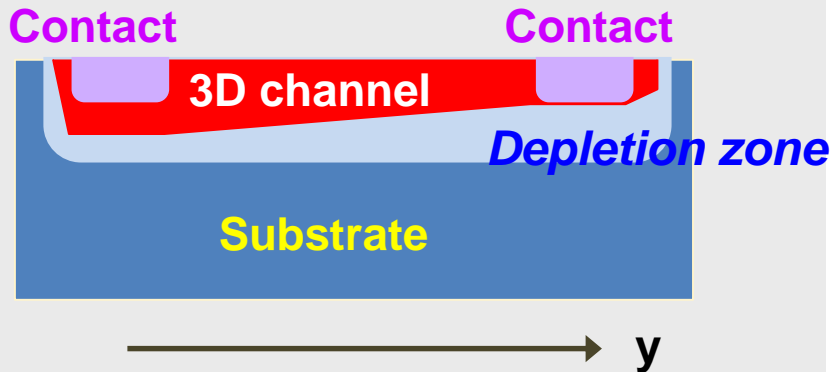
**Heterostructure based Quantum Well Hall Sensor
(III-V)**



Epitaxial AlGaAs/InGaAs/InAs heterostructure (MBE) laterally defined by isolation implant

2D active layer thickness typ. 8-15 nm

- **Standard 3D Hall sensor**
(GaAs, InAs, InGaAs, Si)

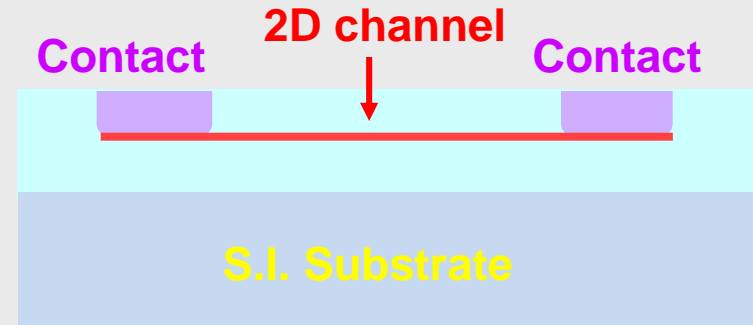


Pinch-off effect (as in MOS transistors)

$n_s(y)$ depends on I_{bias} and T

- $K_H = 1/en_s$ @ $y=L/2$
- Not homogenous: **issue for “spinning current” modulation**
- Also: larger thermal drift
- + carrier freeze-out at low T in Si

- **Quantum Well Hall Sensor**
(Heterostructure based on GaAs, InP,...)



No pinch-off:

$n_s(y) = n_{s0}$ constant vs I_{bias} and y

- Very homogenous electron density
- Excellent temporal stability
- Very weak K_H thermal drift
 $S_T \approx -100 \text{ ppm/}^\circ\text{C}$

Different types of Hall plates: features, advantages and drawbacks

1. Silicon based Hall sensors

Active layer = n-type Si on top of bulk p-type Si

- Various galvanomagnetic effects:
 - Magnetoresistance, non-linearity, planar Hall effect (PHE), piezoresistance
- Suited for integration with CMOS electronics
 - Behavior of IC at high field ?*
- Suited for **monolithic three-axis magnetometers +++**

2. InSb or InAs based sensors

Active layer = μm thick highly doped n-type layer

- Degenerate semiconductor
- Actual mobility much lower than for undoped material
- Low sensitivity, need for a large biasing current (10-100 mA)
- Industrial / small batch

3. Quantum Well Hall Sensors

Active layer = 10 nm thick QW in a III-V heterostructure, + Remote "delta"-doping

- Std RT mobility 7000 cm^2/Vs
- Biasing current 0.2–0.5 mA typ.
- Requires elimination of backgating phenomenon
- Industrial pHEMT technology available from III-V foundry on GaAs substrate

Materials characteristics		
Materials	Bandgap (eV)	Mobility (cm^2/Vs)
Si	1.12 **	1400 *
InSb	0.17	77000 *
InAs	0.35	40000 *
GaAs	1.42	8600 *
$\text{In}_{0.2}\text{Ga}_{0.8}\text{As}$	1.3	7000

(*) For undoped material
(**) Indirect bandgap

Pseudomorphic heterostructure (AlGaAs/InGaAs/GaAs system)

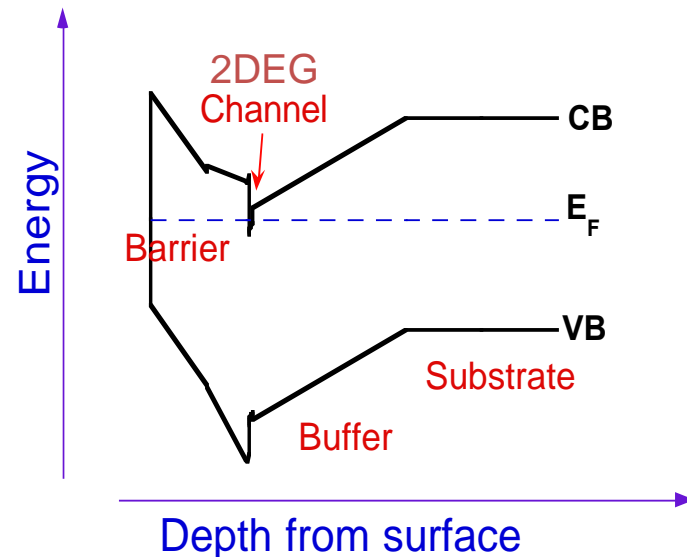
- Buried 2DEG (2D Electron Gas)
- Designed for precision current sensing - 4th gen. being developed
- Batch process:
 - for production: 150 mm GaAs wafers
 - for R&D: 3" and 100 mm GaAs wafers



Features:

- Cross sensitivity $K_H = 700 \Omega / T \pm 5\%$
- Very low thermal drift $S_T \approx -40/-60 \text{ ppm}/^\circ\text{C}$
- Magnetic sensitivity $0.1 - 1 \text{ V/T typ.}$
- Noise PSD $S_B \text{ a few nT}/\sqrt{\text{Hz}}$
- Low raw offset $\pm 3\sigma \leq \pm 1.4 \text{ mT}$
- The offset can be dynamically canceled through SCMT down to $<100 \text{ nT}$ for a magnetometer with 30 mT F.S.
- Temporal stability validated by $>100\text{M}$ Hall plates in ANSI electricity meters since 1999 (class 0.2%)

Band diagram of the heterostructure



Comparison high-mobility 3D versus QWHS Hall probes



Specs:

3D devices

QWHS

Sensor type	AREPOC		ITRON V50 series		
	LHP-Mx series	HHP-Vx series			
Magnetic field range	0 - 33	0-5	0-33	0-5	[T]
Temperature range	1.5 - 350	1.5 - 350	0.03 – 420 (450)		[K]
Intrinsic sensitivity K_H	0.25	2.5	700		[Ω/T]
Sheet carrier density n_s	2.5E+15	2.5E+14	9.0E+11		[cm-2]
Nom. biasing current I_N	20	10	0.07 - 0.14	0.28	[mA]
Sensitivity at I_N	> 5	>50	50 - 100	200	[mV/T]
Signal at nominal induction	> 165	> 250	1650	1000	mV
Offset resistance R_{offset} (3S)	0.005	0.020	0.7		[Ω]
Equivalent magnetic offset B_{offset} (3S)	20	8	1		[mT]
Input resistance R_{in} @ 300 K	4	60	3200		[Ω]
Dissipated power @300K, small B $P = R_{in} \cdot I_N^2$	1.6	6	0.015-0.060	0.25	mW

Effect of offset:

$$\begin{aligned}
 V_{out} &= V_H + V_{offset} \\
 &= K_H \cdot I_{in} \cdot B + R_{offset} \cdot I_{in}
 \end{aligned}$$

Equivalent magnetic offset

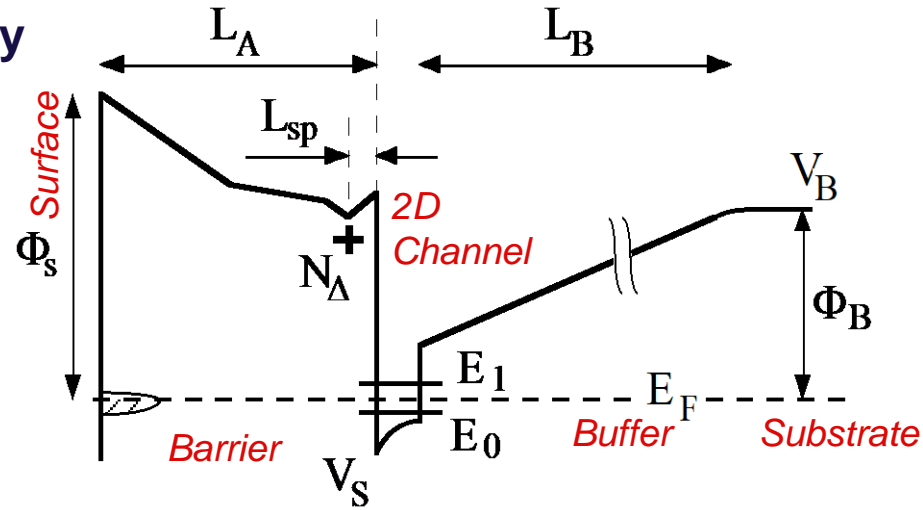
$$B_{offset} = R_{offset} / K_H$$

Black: directly taken from specs

Blue: calculated from specs

- Thermal drift of the magnetic sensitivity

$$S_T \circ \frac{1}{K_H} \times \frac{dK_H}{dT} = - \frac{1}{n_s} \times \frac{dn_s}{dT}$$



By differentiating the $V(z)$ equation:

$$\frac{dn_s}{dT} \gg \frac{e_s}{e L_A} \times \frac{dF_s}{dT} - k_B f(n_s, T) + U_0 \times \frac{1}{e_s} \frac{de_s}{dT}$$

Thermal drift of the surface barrier energy

Major contributor to S_T (85%)

2D Quantum effects

Permittivity variation with T

Small effects

with $U_0 \gg F_s$

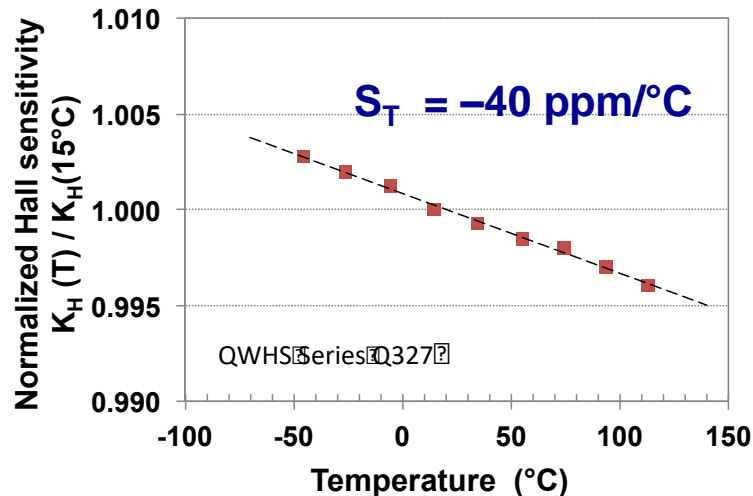
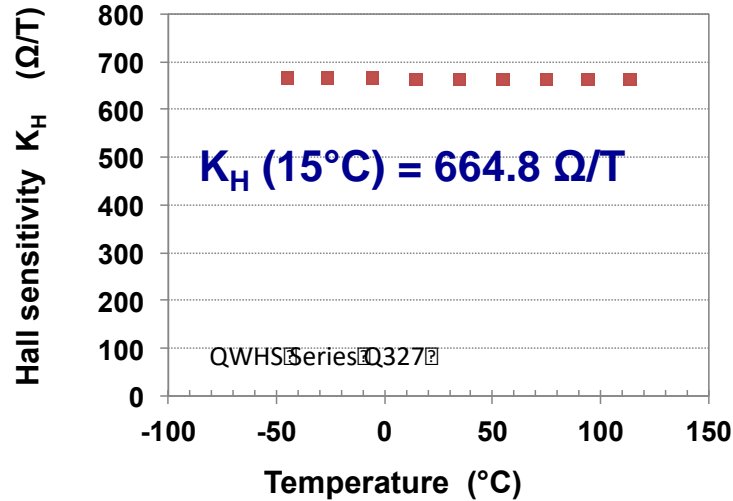
The thermal drift of the sensitivity is mostly controlled by the surface barrier energy

Farah Kobbi's PhD thesis 1996

QWHS Hall probe versus temperature

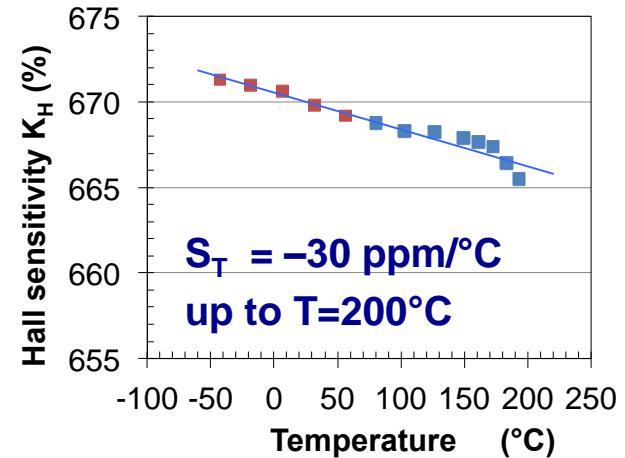
Hall sensitivity vs temperature

Thermal drift: -40 ± 20 ppm/°C in the extended industrial temperature range



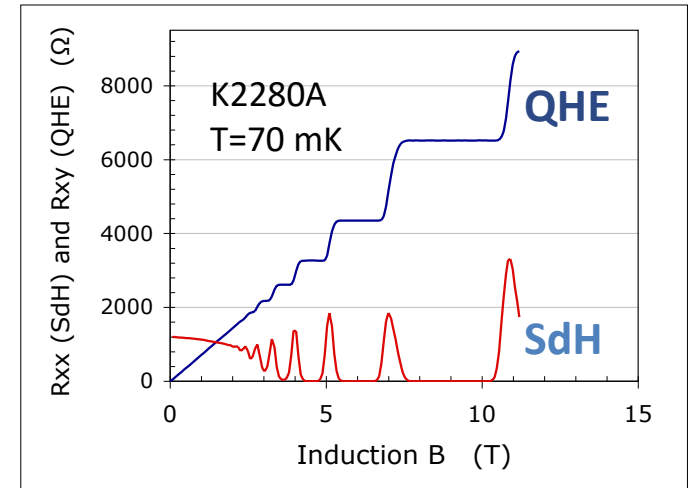
Temperature range

T_{max} at least 200°C when using a Hi-Res

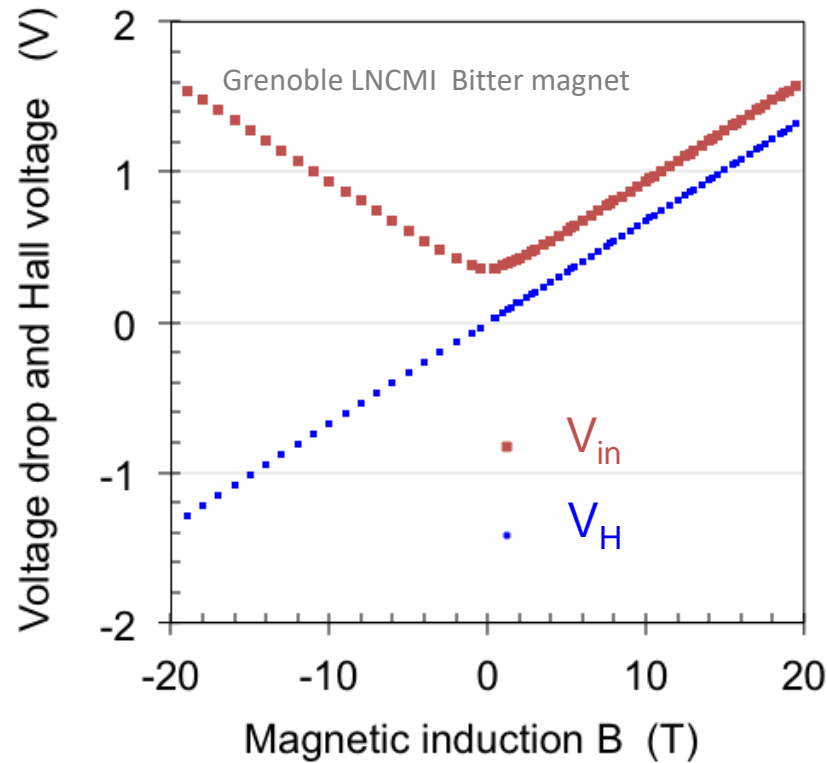


Operation demonstrated at 70 mK

Beware!
QHE at high field

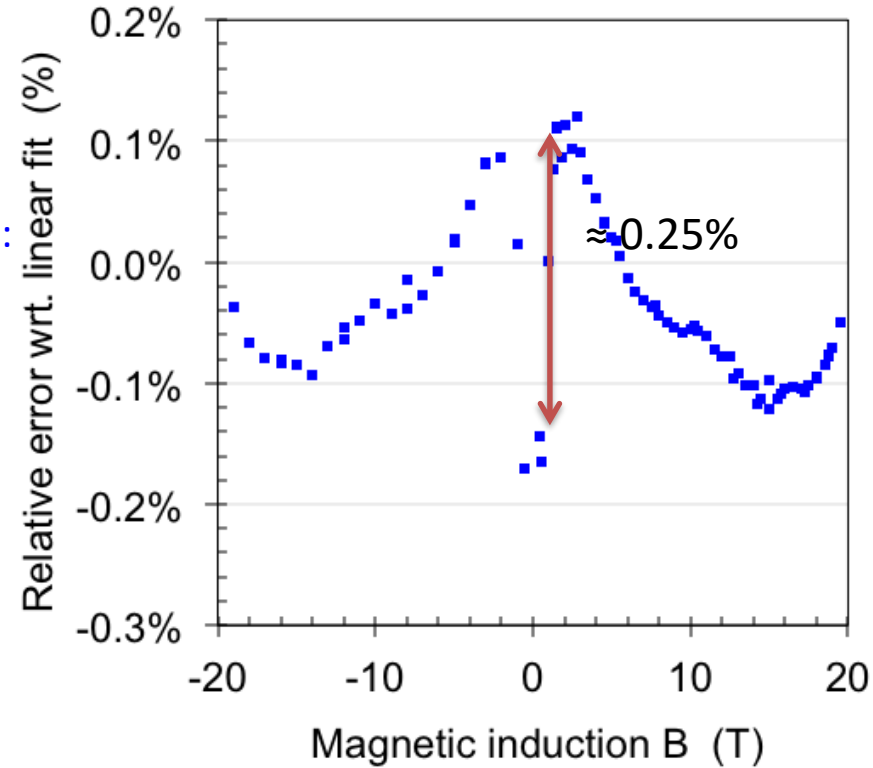


Hall voltage and ohmic voltage drop



Experiment:
22T Bitter
magnet,
LNCMI
Grenoble

Relative error vs. linear fit



$$I_{in} = 100 \mu\text{A}$$

$$\text{Linear fit: } K_H = 678.3 \Omega/\text{T}$$

$$R_{\text{offset}} = -0.6 \Omega$$

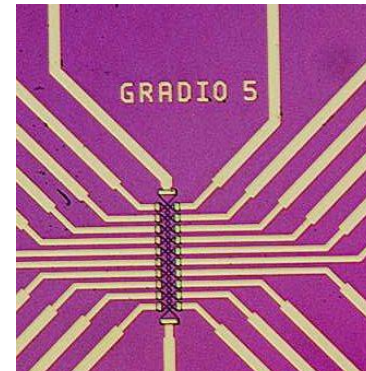
$$e = \frac{V_H^{\text{exp}} - V_H^{\text{fit}}}{V_H^{\text{fit}}}$$

Linearity within $\pm 0.15\%$ of the magnet calibration

Hall based sensors: a broad range of device designs

Various QWHS designs developed by ITRON and LSI

- Processed at Thales R&T (S. Xavier/ J. Cholet / Raphaël Aubry)
- Optical lithography – finest structures in the μm range – 3 metal levels for interconnections
- HTC superconductors, microbead detection, characterization of microstructured magnets, Scanning Hall Probe Microscopy, etc ...



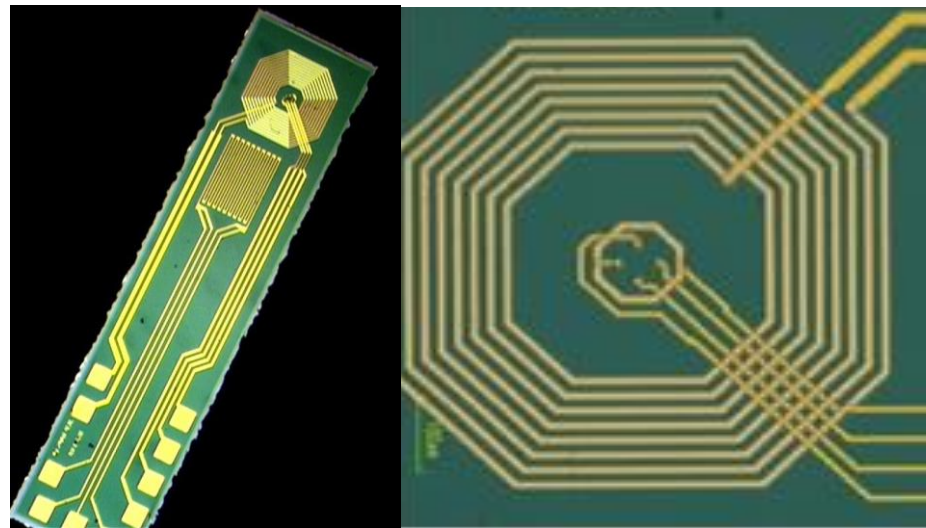
Hall array

T.Klein et al,

PRL 105, 047001 (2010)



Scanning magnetometer



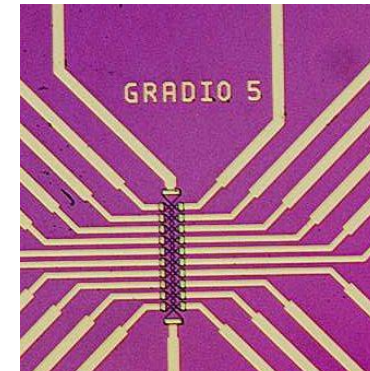
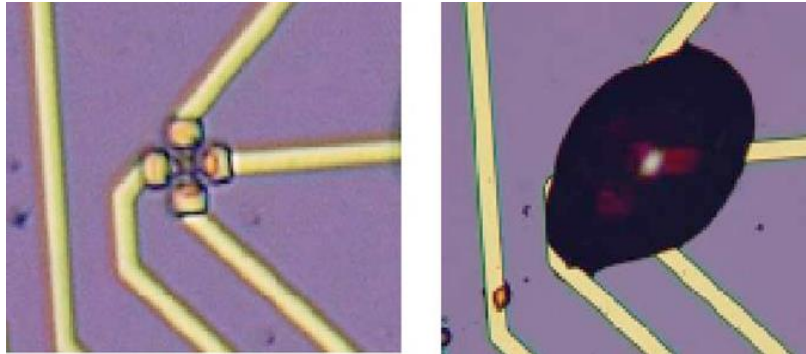
On chip Hall sensor based AC susceptometer

MI Dolz et al, Phys. Rev. Lett. 115, 137003 (2015)

Hall based sensors: a broad range of device designs

QWHS Hall plate with $2\mu\text{m}$ nominal size for investigating the violation of the FDT theorem in ferrofluids

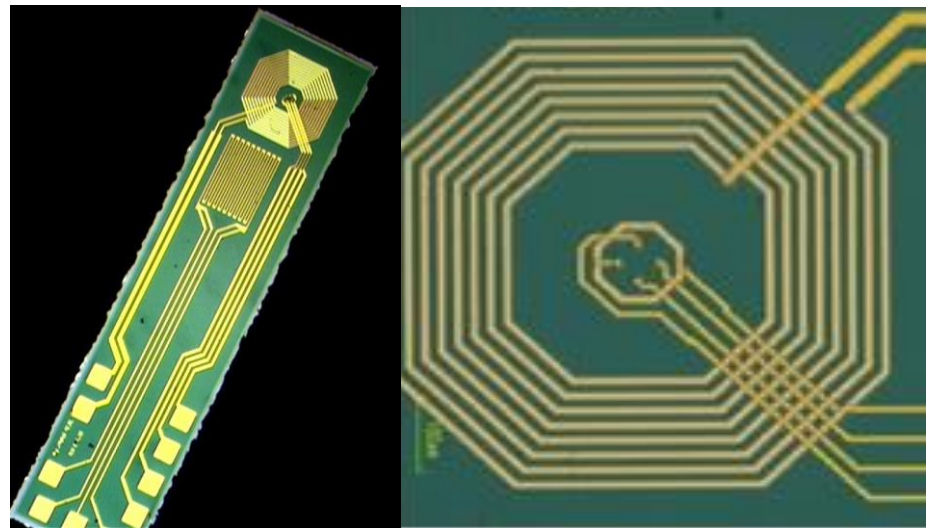
Komatsu et al.,
PRL **106**, 150603 (2011)



Hall array
T.Klein et al,
PRL **105**, 047001 (2010)



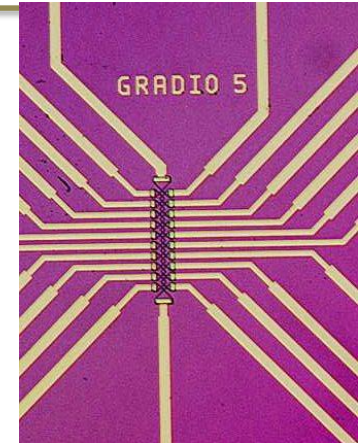
Scanning magnetometer



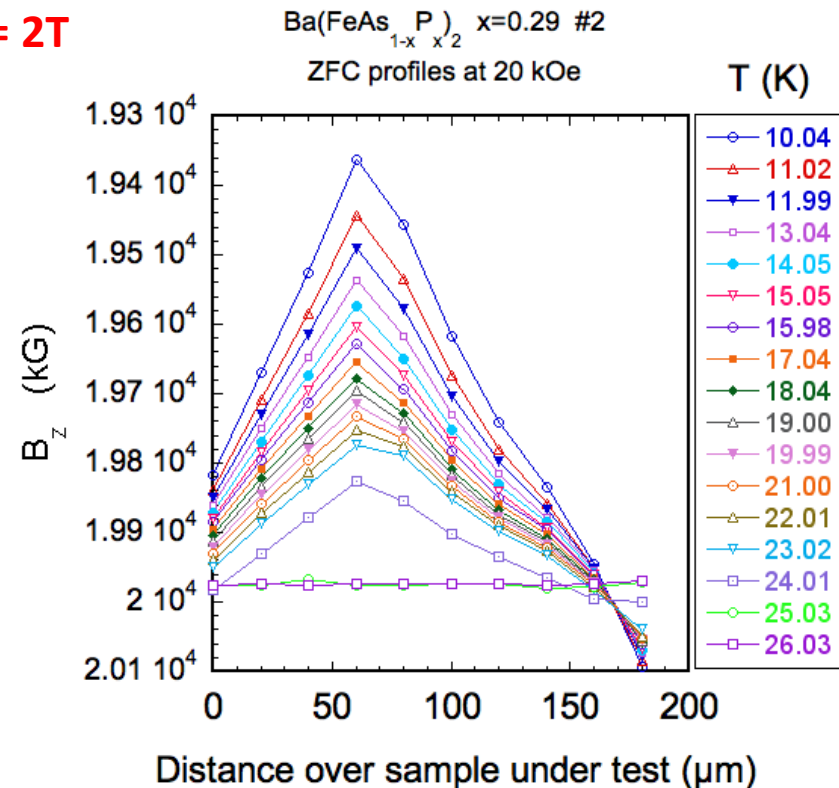
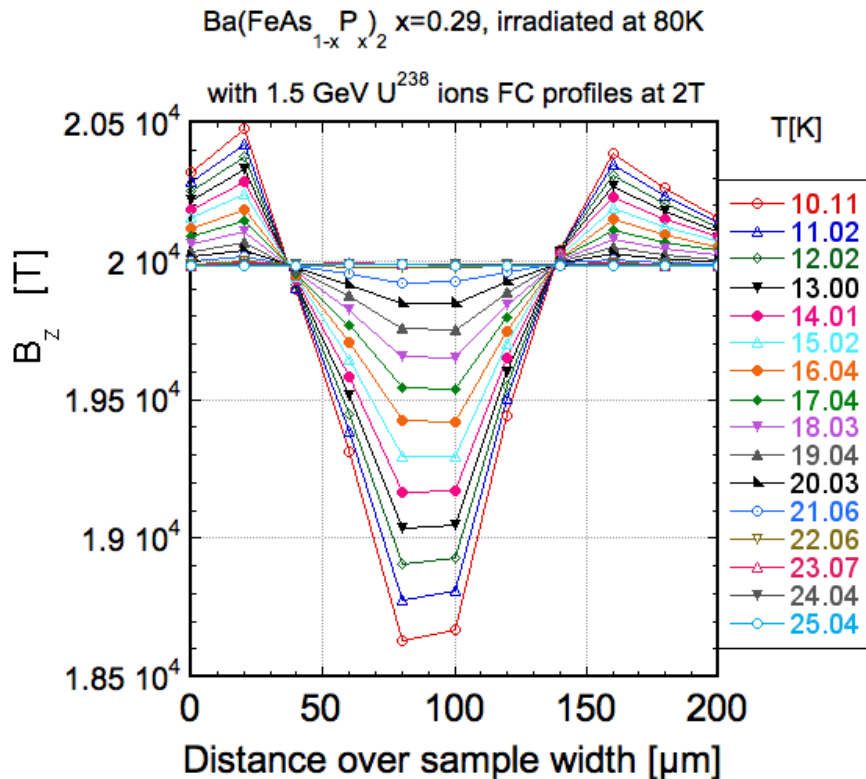
On chip Hall sensor based AC susceptometer
MI Dolz et al, *Phys. Rev. Lett.* **115**, 137003 (2015)

Investigation of topological superconductivity in substituted Iron Pnictides

- BFAP: $\text{Ba}(\text{FeAs}_{1-x}\text{P}_x)_2$ (Courtesy M. Konczykowski, LSI, Polytechnique)
- Needs sensitivity matching and stability in 4 μm wide Hall array in the 0-2T range



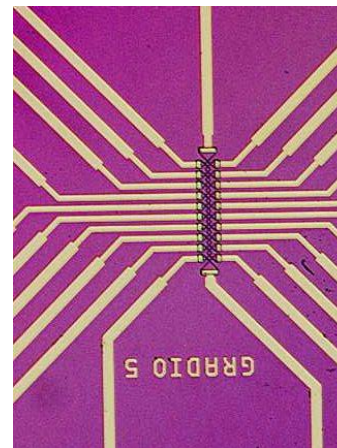
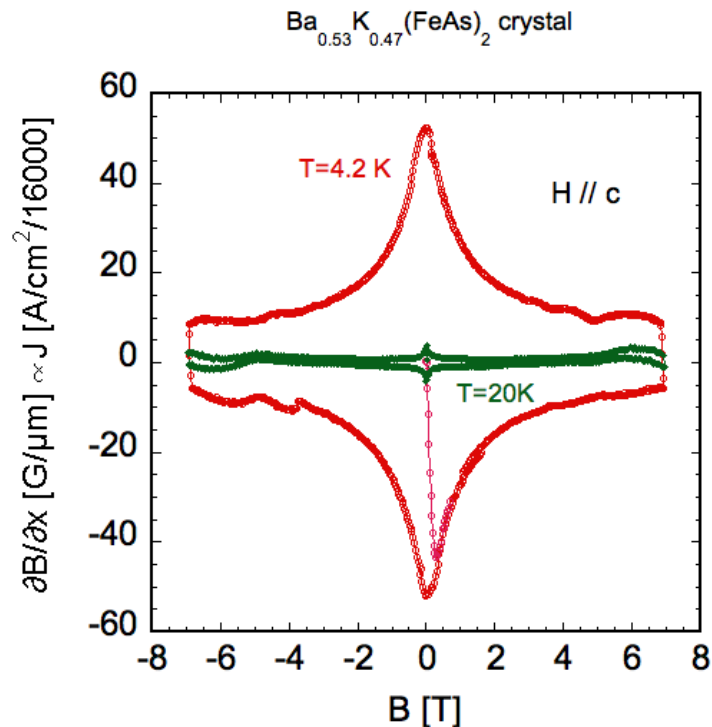
Measurements
around **B = 2T**



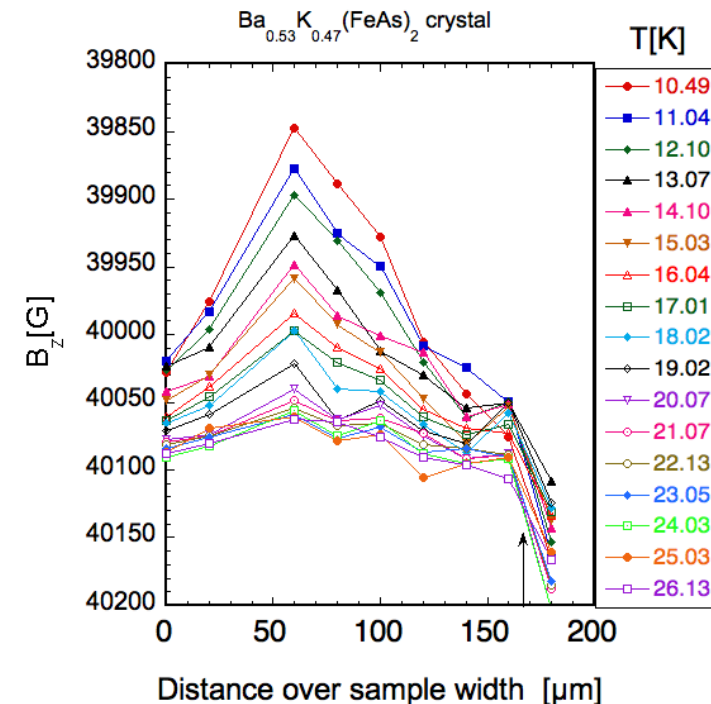
Investigation of topological superconductivity in substituted Iron Pnictides

- BKFA: $\text{Ba}_x\text{K}_{1-x}(\text{FeAs})_2$ (Courtesy M. Konczykowski, LSI Polytechnique)
- Needs sensitivity matching and stability in 4 μm wide Hall array in the 0-8T range

Magnetic field cycles -8T – +8T



Fine measurements around $B = 4\text{T}$



Basic quantities

- Sheet electron density (2D device) n_S *intrinsic 2DEG density*
- Sheet electron density (3D device) $n_S = n_{3D} \times t$ *3D electron density x thickness*
- Electron mobility ($v_d = \mu_n \cdot F$) μ_n *depends on material, doping, temperature, ...*

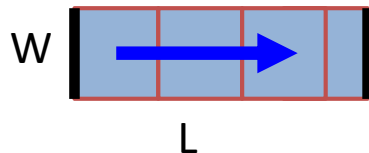
- Intrinsic Hall cross-sensitivity $K_{H0} = 1 / e n_S$, unit = Ω / T

- Output sensitivity $V_{H0} / B = K_{H0} \cdot I_{bias}$ unit = V / T

- 2D resistivity / resistance per square $R_{sq} = 1 / (e n_S \cdot \mu_n) = K_H / \mu_n$ (Planar devices)
- Input or output resistance $R_{in} = G_R \cdot R_{sq}$

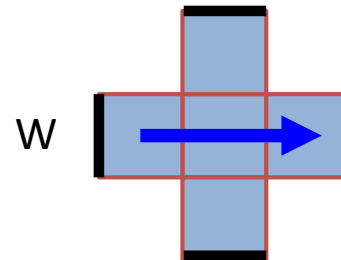
• Rectangular device:

$$G_R = L/W = \# \text{ of squares } N$$



$$L/W = 3.5$$

• Non rectangular device: Effective # of squares:



$$N = L/W = 3 \text{ but}$$

$$G_R = (L/W)^* \approx 2.72 < 3$$

Origin of the geometric factor

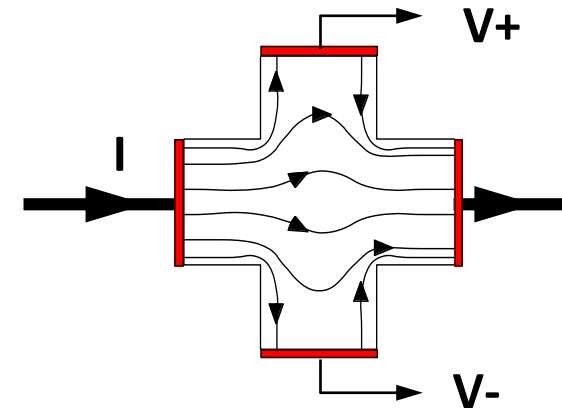
- **Short channel device ($L/W = 2.5$, $G_R \approx 2.2$):**

the active zone is shunted

by the lateral contacts ! $G_H \approx 0.90$

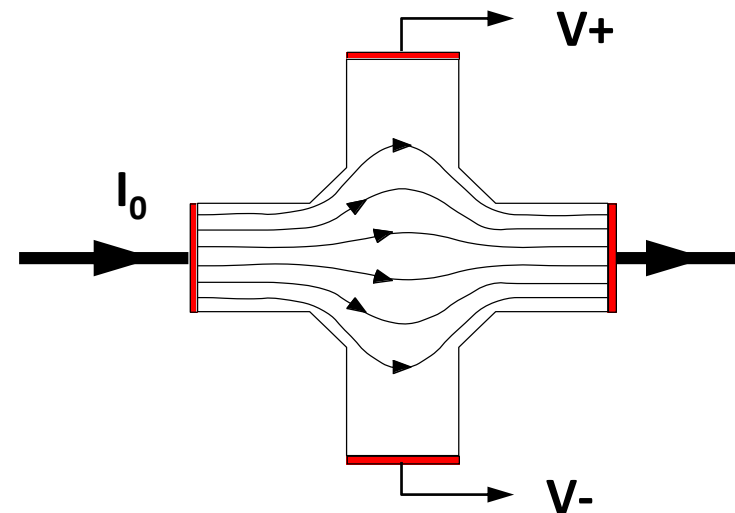
Side effects

- Non-linearity when B large
- Increased noise

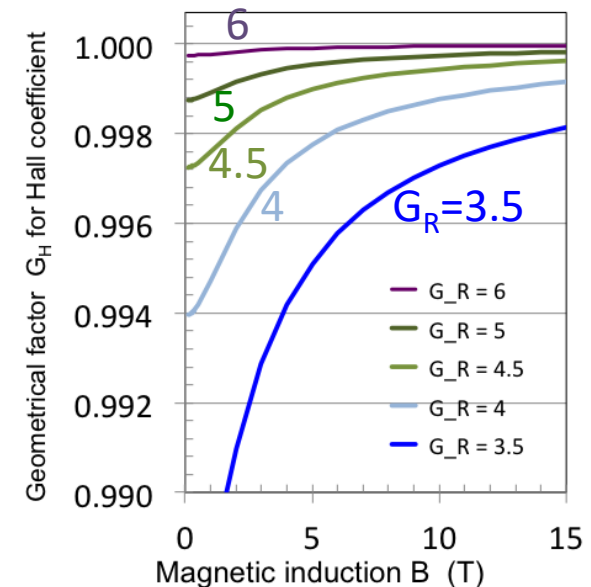
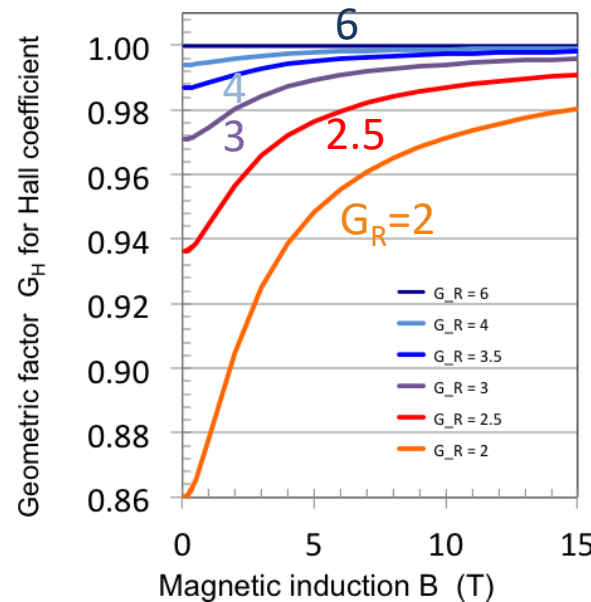
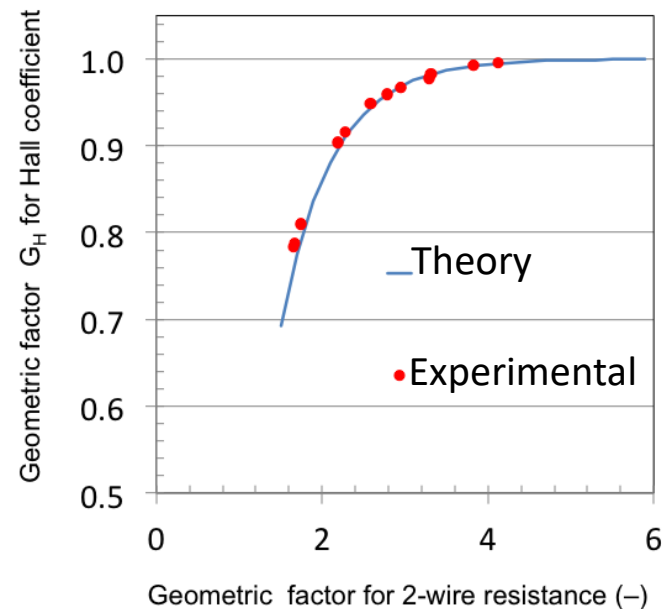


- **Long channel ($L/W=4.5$, $G_R =4$)**

- Geometric factor $G_H=0.99$
- Better linearity



- If the aspect ratio $G_R = R_{in} / R_{sq}$ of the Hall plate is too low (arms too short), then a geometric factor G_H appears in the Hall factor: $K_H = G_H \cdot K_{H0} = G_H / en_{s0}$
- The geometric factor of the resistance (aspect ratio) should be kept large: $G_R \geq 4$, so that G_H remains very close to 1
- Otherwise the geometric factor G_H for the Hall sensitivity would become dependent on B: $K_H = G_H(B) \cdot K_{H0}$



Geometric factors: G_H vs G_R
for devices with 4-fold symmetry

Hall geometric factor $G_H(B)$ for various G_R values

Linked to *time-reversal invariance* of electromagnetism → microscopic reversibility

Onsager: symmetry of transport coefficients (*resistivity tensor, piezoresistivity tensor, etc.*)

Macroscopic reversibility in a 4-contact device

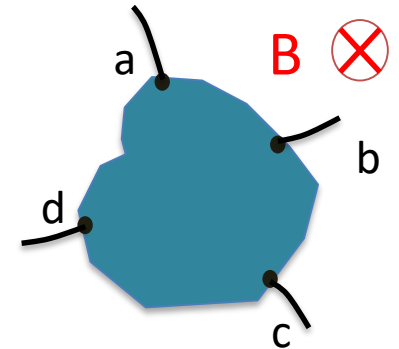
- Permutation of bias and sense:

Assumes that the magnetic field B is reversed in the operation (odd vector)

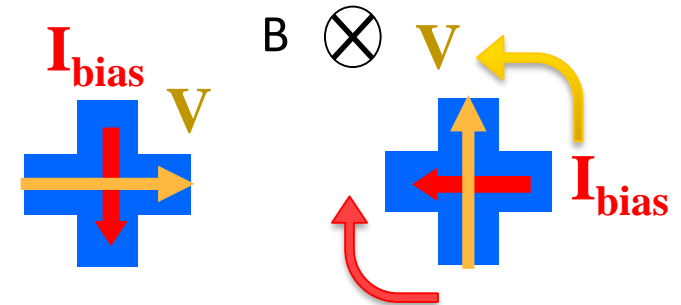
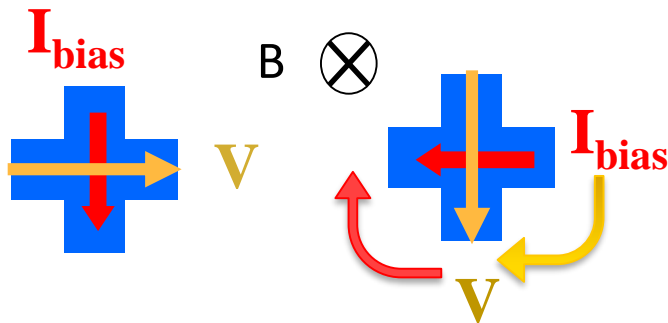
Sample et al., JAP 61, 1079 (1987)

$$R_{ac, bd} \circ \frac{V_{bd}}{I_{ac}}$$

$$R_{ac, bd} = R_{bd, ac}$$



For practical purposes:



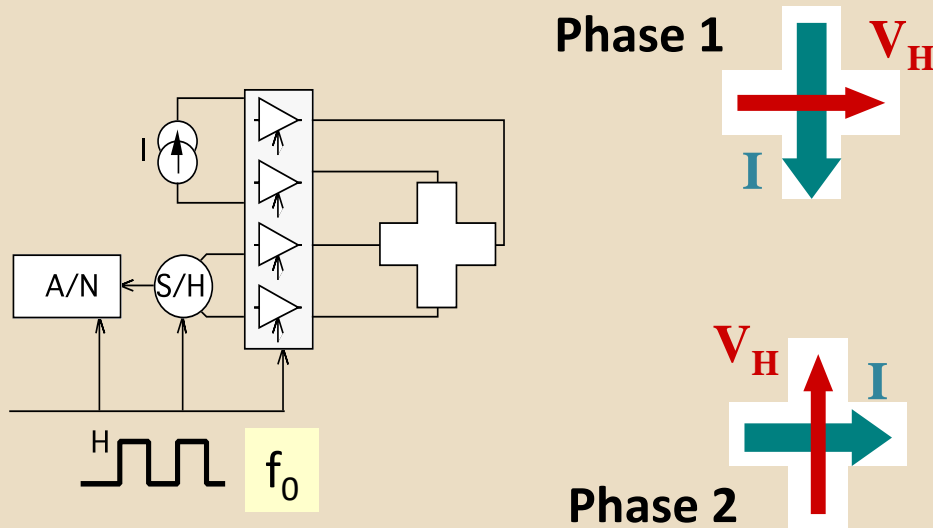
- True rotation of biasing and sensing contacts:

$$\begin{matrix} V_{\text{Hall}} & \rightarrow & V_{\text{Hall}} \\ V_{\text{offset}} & \rightarrow & -V_{\text{offset}} \end{matrix}$$

- Antirootation of biasing and sensing contacts

$$\begin{matrix} V_{\text{Hall}} & \rightarrow & -V_{\text{Hall}} \\ V_{\text{offset}} & \rightarrow & V_{\text{offset}} \end{matrix}$$

Basic 2 phase spinning current method



• Offset suppression:

$$V_{out_1} = K_H I B + R_{offset} I$$

$$V_{out_2} = K_H I B - R_{offset} I$$

• LF noise suppression:

$$V_{out_1} = K_H I B + R_{offset} I + r_n I + v_n^{th}$$

$$V_{out_2} = K_H I B - R_{offset} I - r_n I + v_n^{th}$$

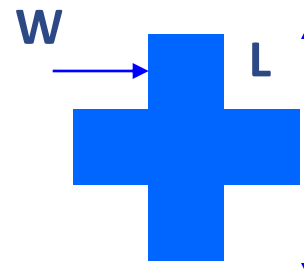
• Principle of offset suppression in Hall measurements

L. Van der Pauw (1958)

• Cancellation of LF noise of Hall sensors

Z. Stoessel and Markus Resch,
Sensors and Actuators **A37-38**, 449 (1993)

• Remained unnoticed for over 10 years



Consequence:

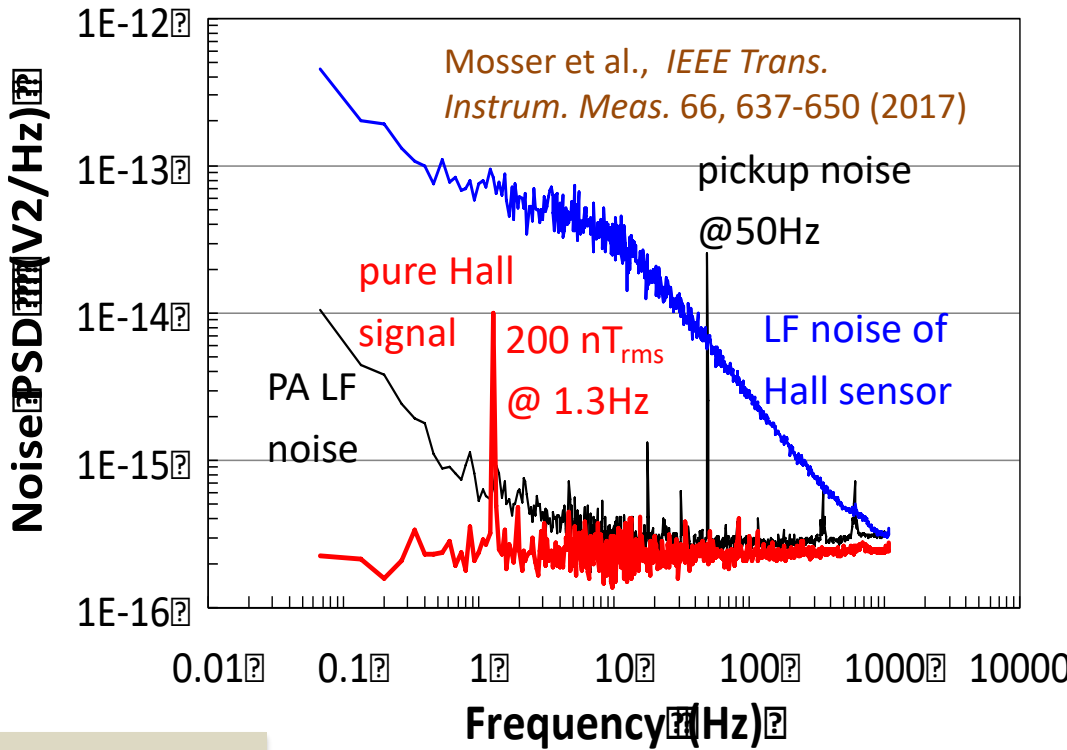
- Design Hall device with fourfold symmetry (e.g. Greek cross)

WHAT SCMT DOES

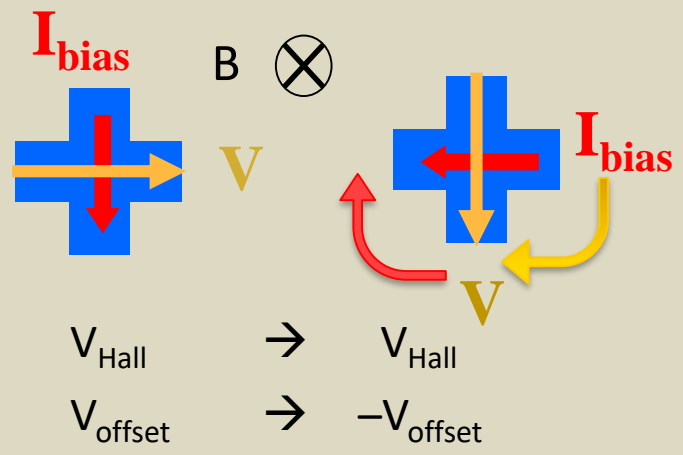
- SCMT effectively cancels the **offset** and **LF noise** of Hall sensors
- Also eliminates the **noise and offset of the whole acquisition chain** (amplifier, interconnects)
- Real-time, broadband

HOW SCMT WORKS

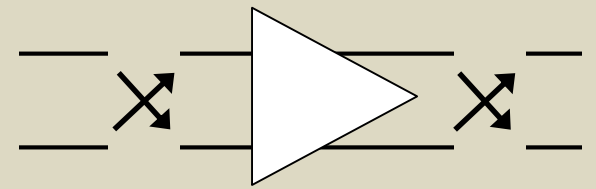
- A combination of 2 principles:



1. Reverse Magnetic Field Reversibility (RMFR)



2. Chopped amplifier for offset suppression

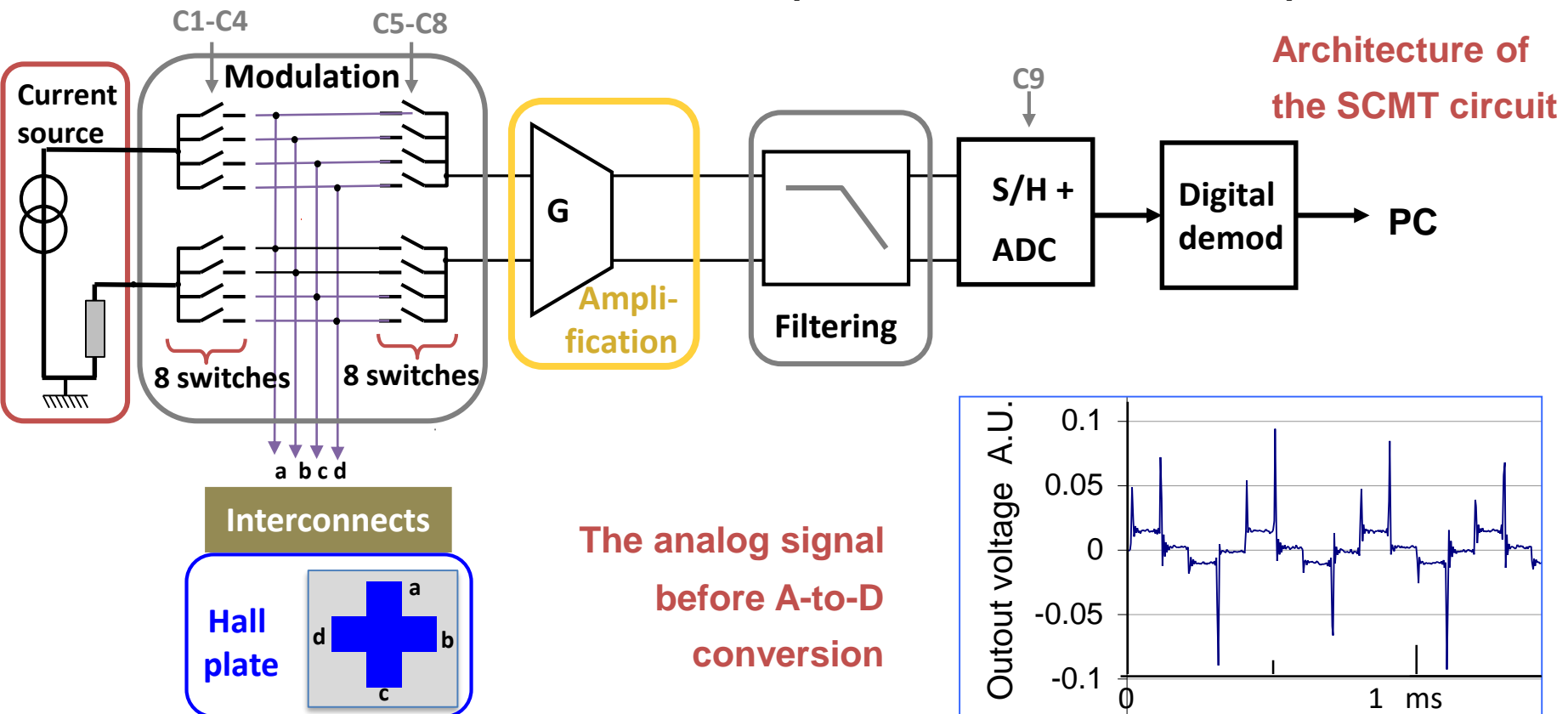


The Spinning Current Modulation Technique (SCMT) -2-

Output signal:

$$V_{out} = G \times \left(\underbrace{V_H}_{\text{HALL PLATE}} + \underbrace{V_{offset}^{Hall}}_{\text{PREAMPLIFIER}} + \underbrace{V_{offset}^{PA}}_{\text{PREAMPLIFIER}} + \underbrace{e_{th}}_{\text{INTERCONNECTS}} + \underbrace{V_{ind}}_{\text{INTERCONNECTS}} + \underbrace{v_{LF}^{Hall}}_{\text{PREAMPLIFIER}} + \underbrace{v_{LF}^{PA}}_{\text{PREAMPLIFIER}} + v_{th} \right)$$

SCMT principle: - By combining 4 successive different configurations, one can suppress all parasitic contributions, excepted thermal noise



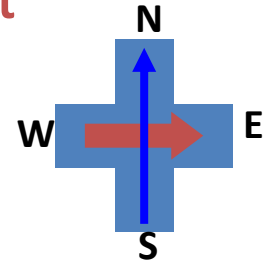
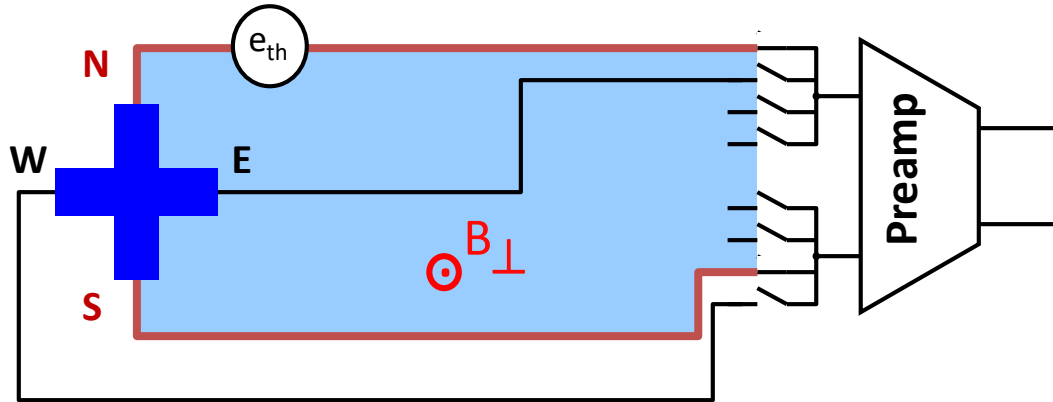
Spinning current circuitry: induced e.m.f. and thermoelectric effect

$$V_{emf}^{NS} = - \frac{dF}{dt} \Big|_{NS}$$

$$= \iint_{area\ NS} \frac{dB}{dt} ds$$

Induced e.m.f.

Voltage sense connected to branch NS

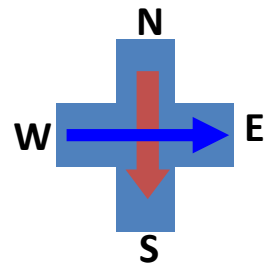
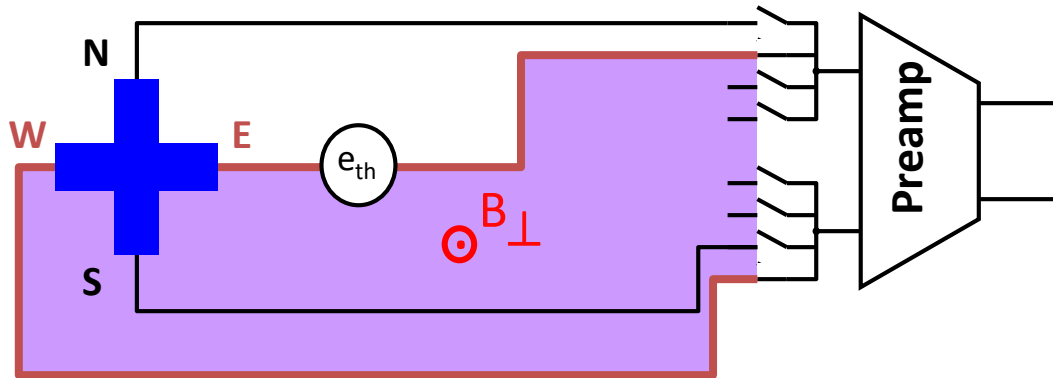


in branch NS: e_{th}^{NS}

Thermoelectric effect

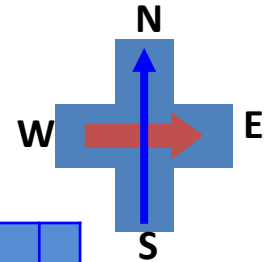
in branch EW: e_{th}^{EW}

Voltage sense connected to branch EW



Hall effect measurement: spinning sequence

- Basic: canceling **offset** and **LF noise** from **Hall sensor** and **preamp**
- Advanced: canceling the **pickup noise** and **thermoelectric effect**



Config #	Hall device				Circuit						
	I+	I-	V+	V-	Hall signal	Hall offset + LFN	Preamp offset + LFN	$\frac{d\Phi}{dt}$	e_{th}	DEM	
1	N	S	E	W	+	+	+	$+V_{EW}$	$+e_{EW}$	+1	
2	E	W	S	N	+	-	+	$-V_{NS}$	$-e_{NS}$	+1	
3	S	N	W	E	+	+	+	$-V_{EW}$	$-e_{EW}$	+1	
4	W	E	N	S	+	-	+	$+V_{NS}$	$+e_{NS}$	+1	
5	N	S	W	E	-	-	+	$-V_{EW}$	$-e_{EW}$	-1	
6	E	W	N	S	-	+	+	$+V_{NS}$	$+e_{NS}$	-1	
7	S	N	E	W	-	-	+	$+V_{EW}$	$+e_{EW}$	-1	
8	W	E	S	N	-	+	+	$-V_{NS}$	$-e_{NS}$	-1	

Suitable sequences

- 1278
- 1368
- 1467
- 2358
- 2457
- 3456

4-phase modulation: choose 2 states among #1-#4 and 2 states among #5-#8

- Optimized spinning **sequence 1278** + demodulation **+1/+1/-1/-1**

Config #	I+	I-	V+	V-	After spinning				DEMO D	After demodulation			
					Hall signal	Hall offset + LF noise	PA offset + LF noise	Pickup noise		Hall signal	Hall offset + LF noise	PA offset + LF noise	Pickup noise
1	N	S	E	W	+	+	+	$+V_{EW}$	+1	+	+	+	$+V_{EW}$
2	E	W	S	N	+	-	+	$-V_{NS}$	+1	+	-	+	$-V_{NS}$
7	S	N	E	W	-	-	+	$+V_{EW}$	-1	+	+	-	$-V_{EW}$
8	W	E	S	N	-	+	+	$-V_{NS}$	-1	+	-	-	$+V_{NS}$

Summation for 4 phases: $4 V_H$ 0 0
0

The offset and LF noise of the Hall sensor,
the offset and LF noise of the preamplifier,
the pickup noise and thermoeffect from the interconnects

are expected to be canceled

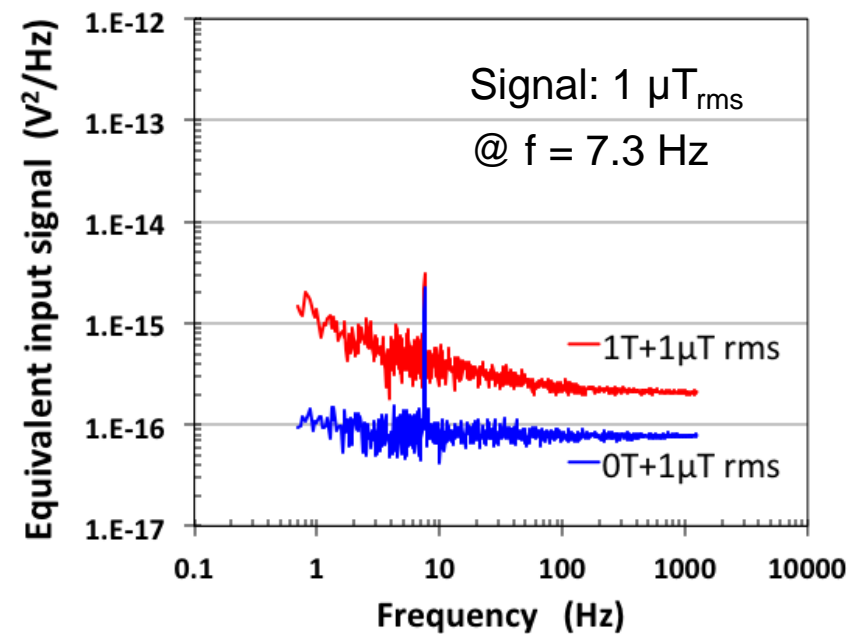
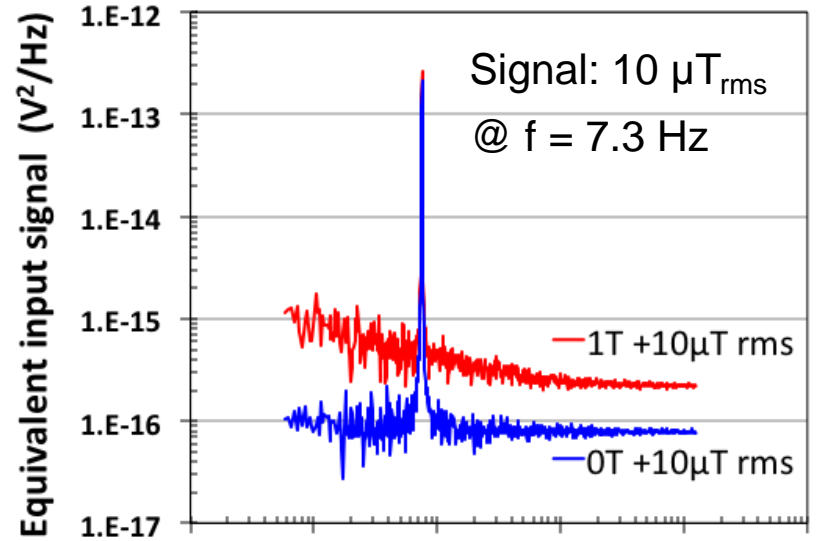
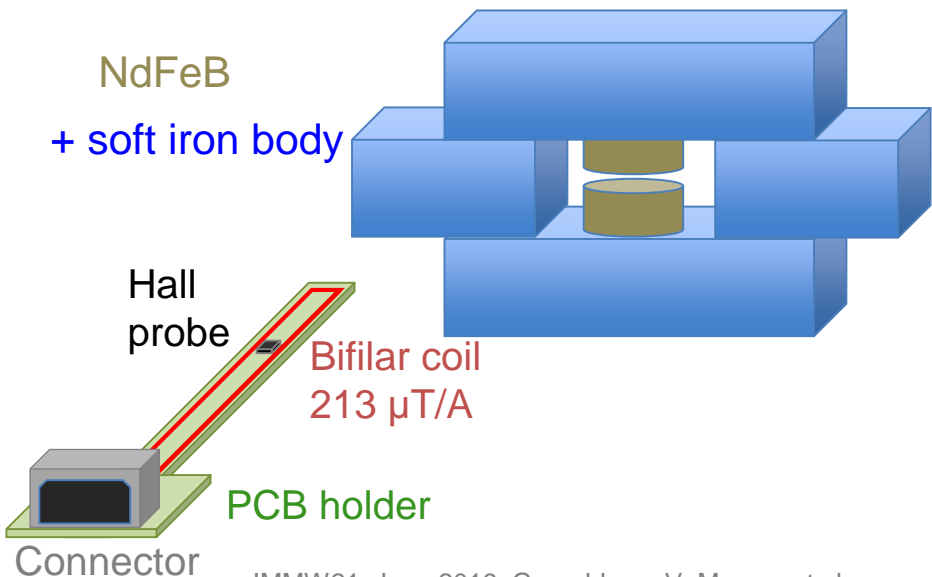
Resolution of Hall microsystem at high field -1-

- **Microsystem Hall sensor head + acquisition board including SCMT (spinning current)**

$K_H \cdot I_{in} \approx 0.095 \text{ V/T}$
 $G_{analog} = 10 \quad / \quad G_{dig} = 4$
 Full Scale = $\pm 6 \text{ T}$
 Resolution $170 \text{ nT @ } B_{DC} = 0 \text{ T}$
 $500 \text{ nT @ } B_{DC} = 1 \text{ T}$

- **Magnetic field source:**

Permanent magnet 1T + bifilar coil



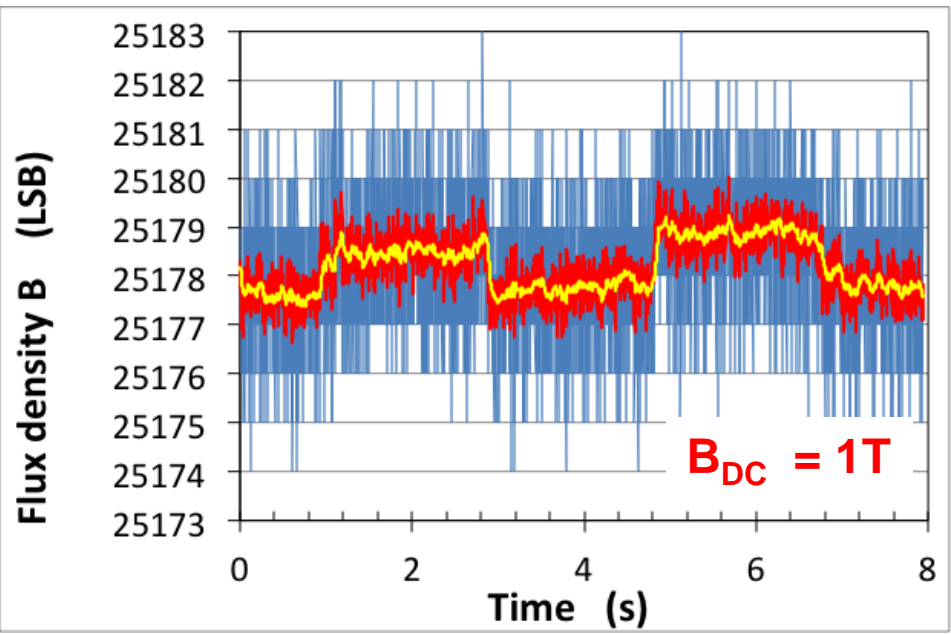
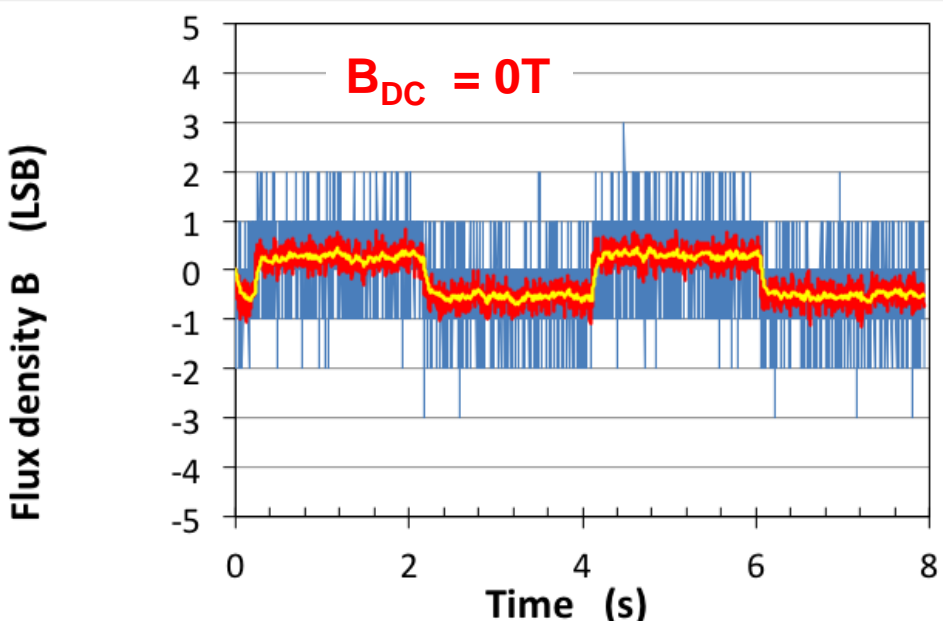
Resolution of Hall microsystem at high field -2-

- In the time domain:**

$B_{AC} = \text{square wave } 30 \mu\text{T}_{p-p}$

Acquisition 10ks/s+ digital filtering

Blue	raw data	($f_s = 2500 \text{ Hz}$)
Red	$t_C = 4 \text{ ms}$	
Yellow	$t_C = 40 \text{ ms}$	



System characteristics:

- $K_H \cdot I_{in} \approx 0.095 \text{ V/T}$
- $G_{analog} = 10 / G_{dig} = 4$
- 1 LSB $\approx 35 \mu\text{T}$
- Full Scale = $\pm 6 \text{ T}$

- Resolution much better than 1 LSB thanks to the dither effect**
- More noise at B = 1T**

Resolution of Hall microsystem at high field -3-

- In the time domain:**

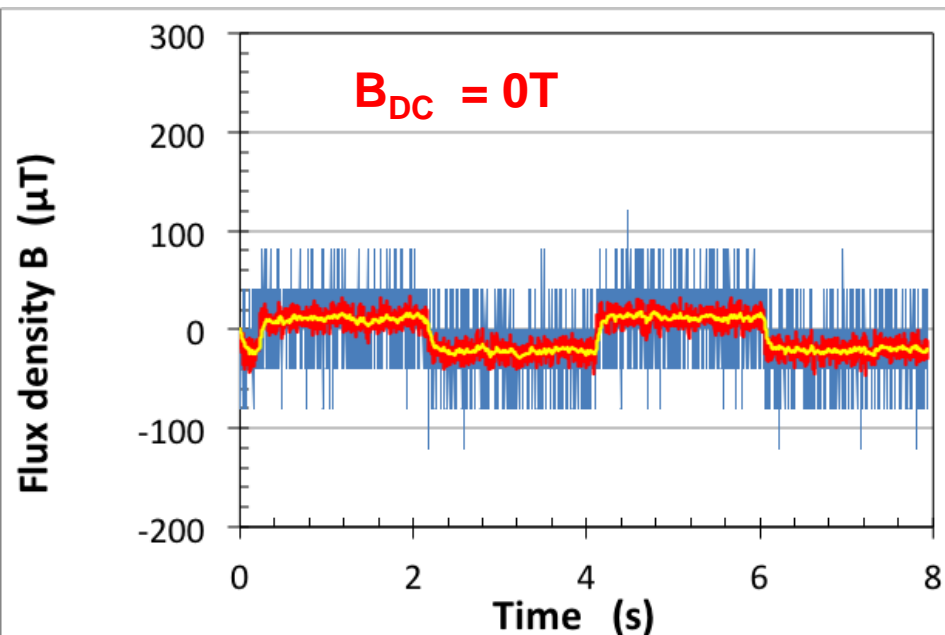
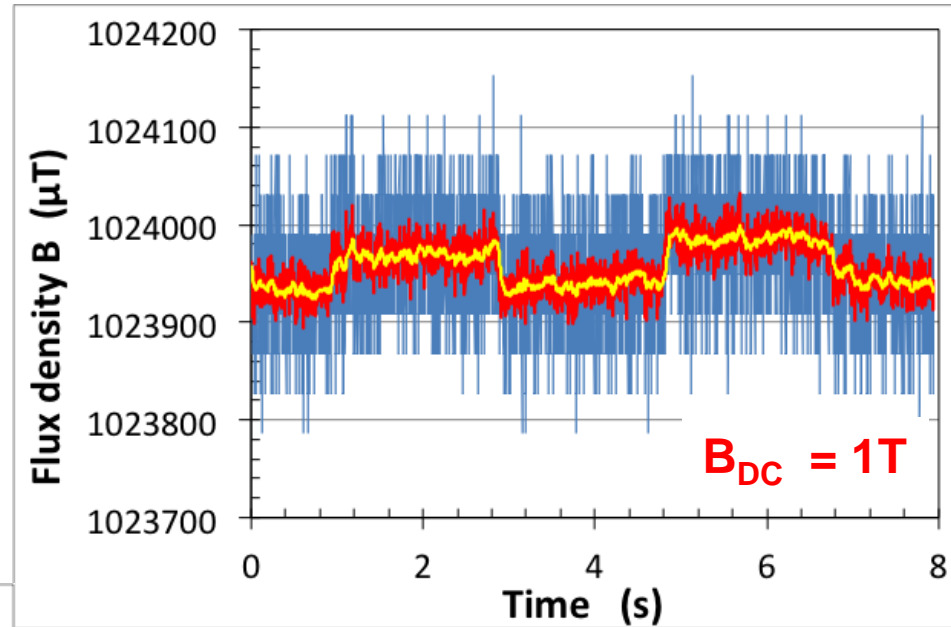
B_{AC} = square wave $30 \mu\text{T}_{p-p}$

Acquisition 10ks/s+ digital filtering

Blue raw data ($f_s = 2500 \text{ Hz}$)

Red $t_C = 4 \text{ ms}$

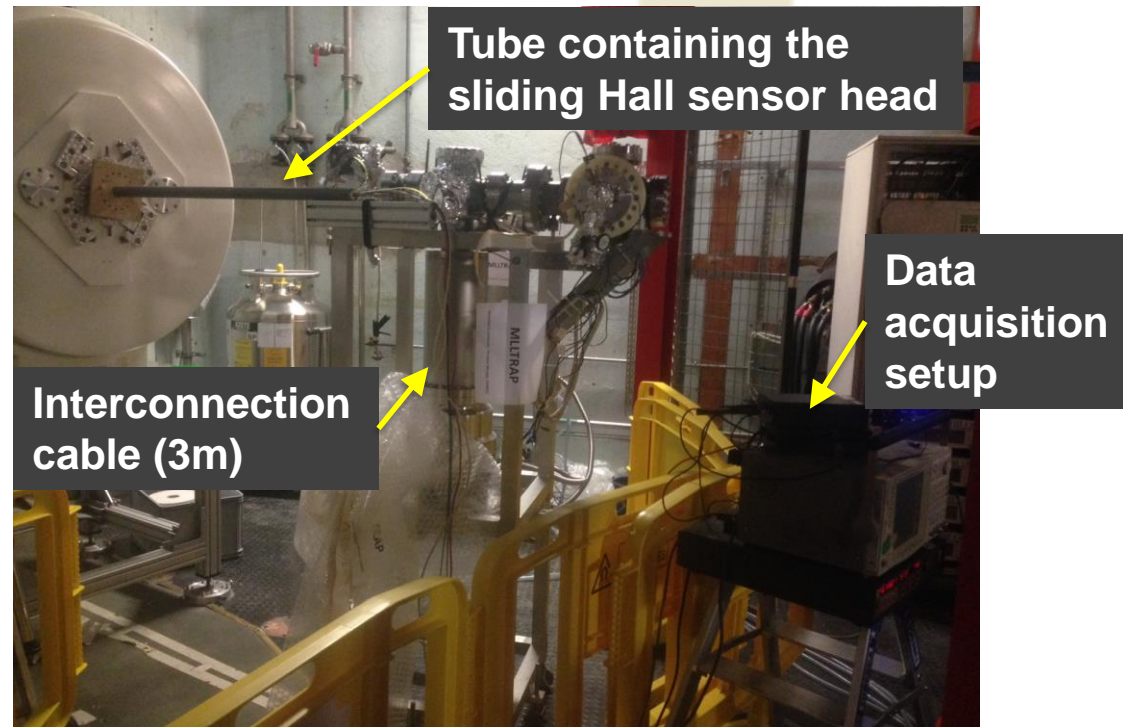
Yellow $t_C = 40 \text{ ms}$



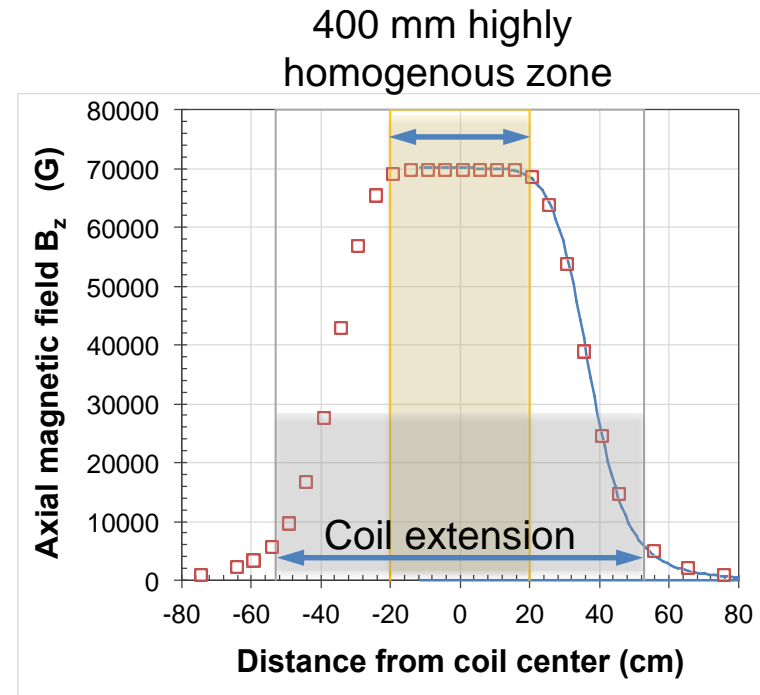
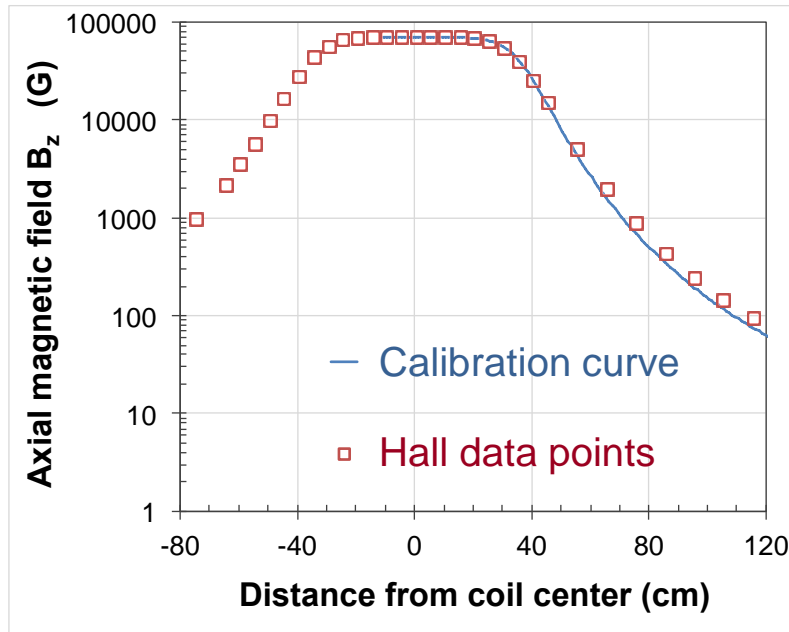
- Full Scale = $\pm 6 \text{ T}$
- The mean signal at $B_{DC} = 0 \text{ T}$ is about $-20 \mu\text{T}$, due to the orthogonal component of the earth magnetic field
- Residual offset / Full Scale at most in the ppm range

Goal:

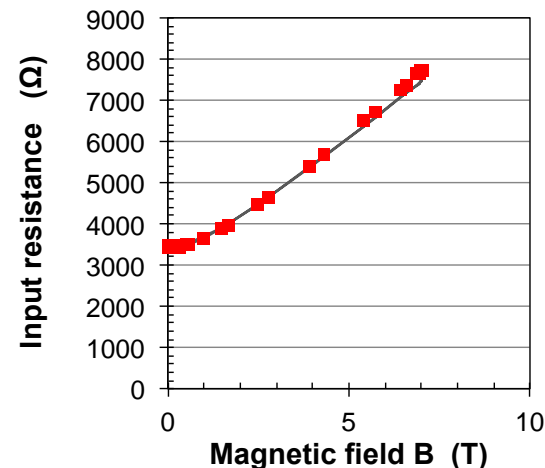
- Profiling the magnetic field along the axis of the MLL-trap superconducting magnet at IPN.
 - Penning Trap using a superconducting magnet (Magnex Scientific) in the persistent mode
- Freely accessible cylindrical cavity along the magnet axis (diam. 10 cm)
- with highly homogenous magnetic field in a 40 cm long region in the magnet center,
 - and decaying magnetic field along the magnet axis



Magnetic field profile along the magnet axis



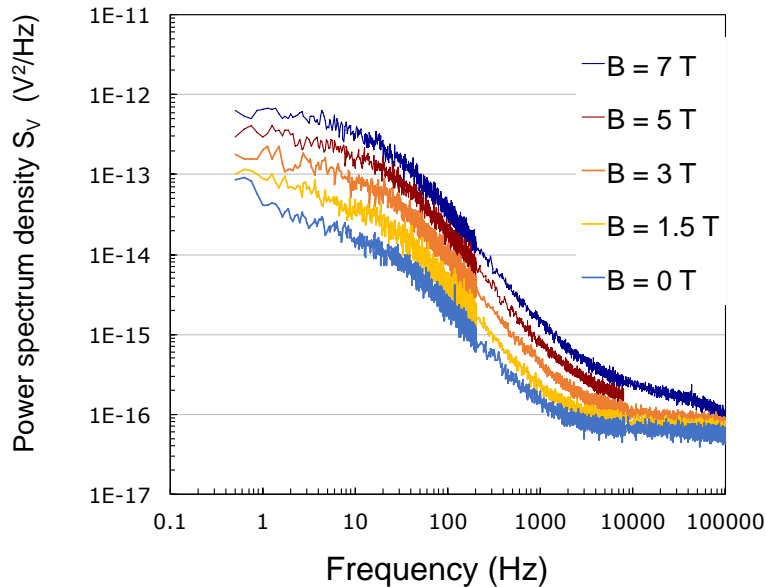
- QWHS Hall plate calibrated around 0.5T using a NMR regulated electromagnet
- B found to be 7.006 T in the plateau region, in close agreement with the calibration curve from the provider
- Stray field determined along the magnet axis



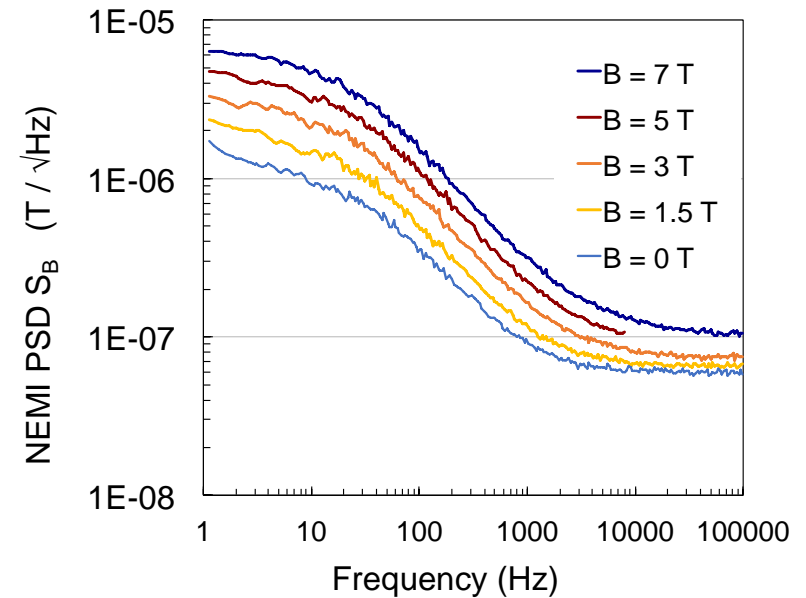
Input resistance vs magnetic induction

Rationale

Use the noiseless stray magnetic field in order to characterize the sensor noise between 0 and 7T.



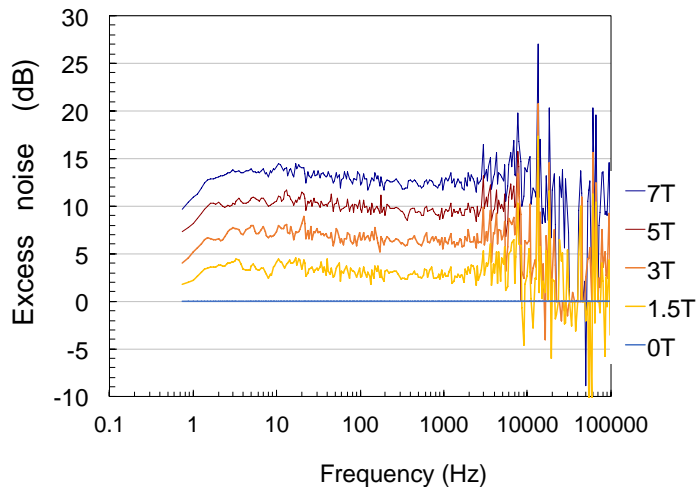
Raw noise spectra
from Fourier transform
analyzer



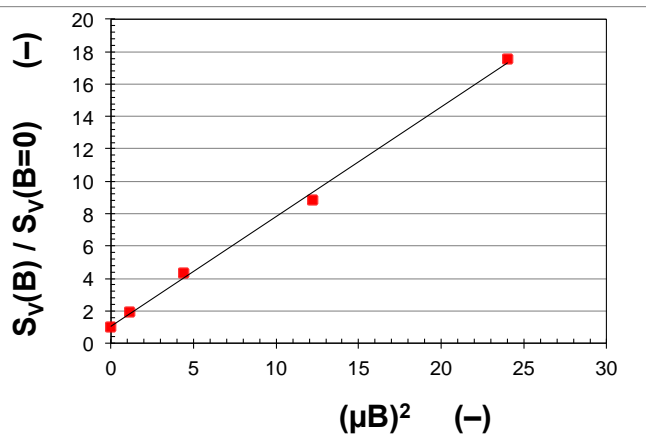
Resulting noise equivalent
magnetic induction (NEMI)
spectra

- Eliminate duplicate data
- Data smoothing
- Deembedding of parasitic impedance ($C_{\text{cable}} = 180 \text{ pF}$)

Noise PSD vs magnetic induction

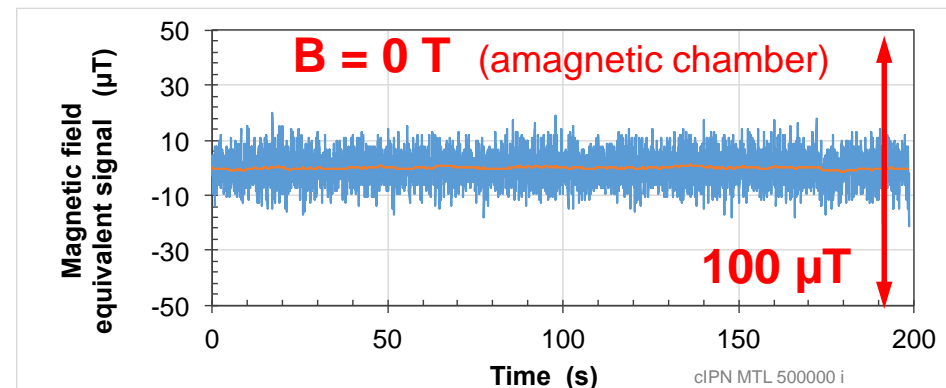
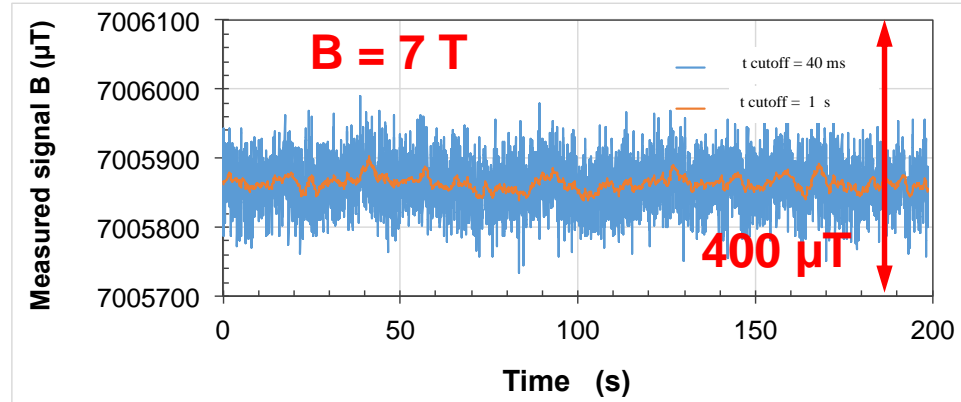


Excess noise vs frequency



Excess noise $\sim 1 + (\mu B)^2$

In the time domain

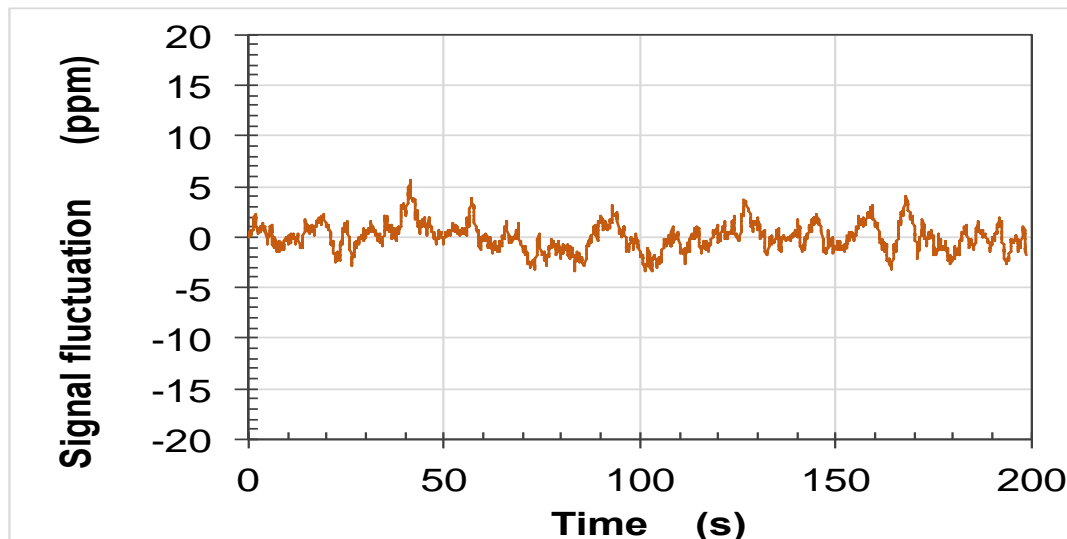


Cutoff frequency: Blue $f_c = 25 Hz$
 Orange $f_c = 1 Hz$

Excess noise $\times 20$ from $B=0T$ to $B=7T$

Hall signal fluctuation at $B = 7\text{ T}$

- QWHS $W = 30\text{ }\mu\text{m}$, room temperature
- Spinning current SCMT with acquisition frequency 10 kHz



$B = 7\text{ T}$

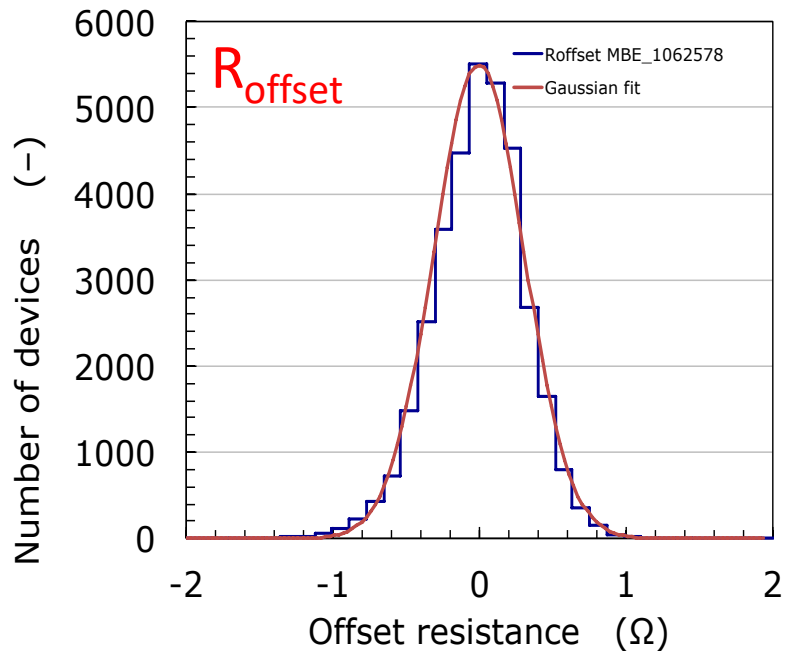
- A few ppm signal fluctuation when $BW = 1\text{ Hz}$
- Dispersion $\pm 3\sigma$ corresponds to $\pm 10\text{ }\mu\text{T}$

CONCLUSION

- For magnetometry and **micromagnetometry applications** at high magnetic field, Quantum Well Hall Sensors may be a good choice
- We demonstrated the capabilities of QWHS
 - for magnetic field metrology in the 0-20T range
 - as well for micromagnetometry at the micrometer level in the 0-8T range
- The temperature range depends on the field strength
 - 70 mK – 200°C demonstrated at low field (≤ 1 T)
 - Quantum Hall Effect oscillations at higher field and $T < \text{a few K}$
- Using the Spinning Current Modulation Technique, a QWHS based microsystem with ± 6 T range shows a resolution better than $1\mu\text{T}$, at least @ $B=1$ T
- A QWHS was characterized between 0 and 7T, using the stray axial field of a Penning trap superconducting electromagnet in persistent mode
- Noise increase $\times 20$ from $B=0$ T to $B=7$ T

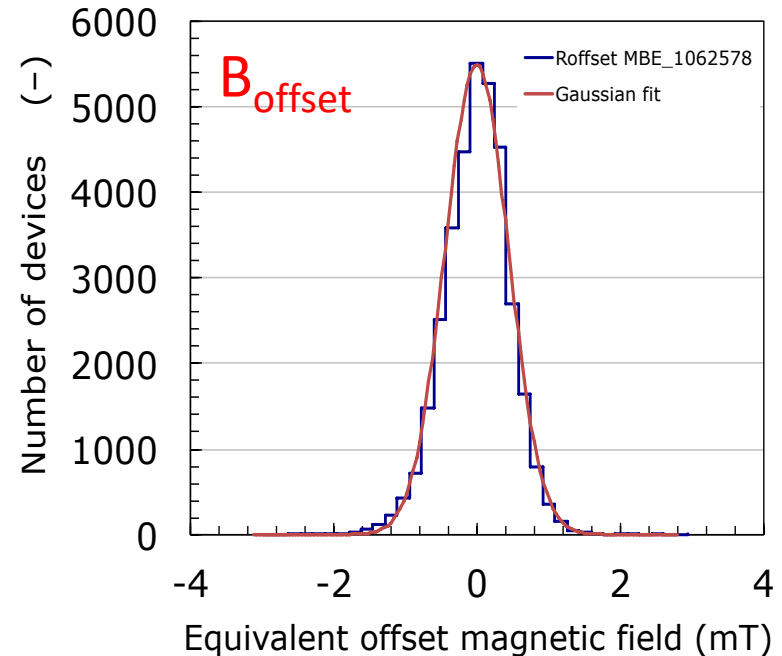


RAW OFFSET OF QWHS SENSORS



$$R_{\text{offset}} : \quad \sigma = 0.33 \, \Omega$$

$$\quad \quad \quad \pm 3 \sigma = \pm 1.0 \, \Omega$$



$$B_{\text{offset}} : \quad \sigma = 0.43 \, \text{mT}$$

$$\quad \quad \quad \pm 3 \sigma = \pm 1.3 \, \text{mT}$$

$$\text{Equivalent misalignment } \Delta L_{\text{eff}} : \quad \sigma = 45 \, \text{nm}$$

Offset distribution over a wafer, 70000 devices (raw data)